Mon. Not. R. Astron. Soc. **000**, 000–000 (0000) Printed 3 March 2016 (MN LATEX style file v1.4)

Stochastic reacceleration of relativistic electrons by turbulent reconnection: a mechanism for cluster-scale radio emission ?

G. Brunetti,[1] A. Lazarian[2]

[1] *INAF/Istituto di Radioastronomia, via Gobetti 101, I–40129 Bologna, Italy*

[2] *Department of Astronomy, University of Wisconsin at Madison, 5534 Sterling Hall, 475 North Charter Street, Madison, WI 53706, USA*

arXiv:1603.00458v1 [astro-ph.HE] 1 Mar 2016

3 March 2016

ABSTRACT

In this paper we investigate a situation where relativistic particles are reaccelerated diffusing across regions of reconnection and magnetic dynamo in super-Alfvenic, incompressible large-scale turbulence. We present an exploratory study of this mechanism in the intra-cluster-medium (ICM). In view of large-scale turbulence in the ICM we adopt a reconnection scheme that is based on turbulent reconnection and MHD turbulence. In this case particles are accelerated and decelerated in a systematic way in reconnecting and magnetic-dynamo regions, respectively, and on longer time-scales undergo a stochastic process diffusing across these sites (similar to second-order Fermi). Our study extends on larger scales numerical studies that focused on the acceleration in and around turbulent reconnecting regions. We suggest that this mechanism may play a role in the reacceleration of relativistic electrons in galaxy clusters providing a new physical scenario to explain the origin of cluster-scale diffuse radio emission. Indeed differently from current turbulent reacceleration models proposed for example for radio halos this mechanism is based on the effect of large-scale incompressible and super-Alfvenic turbulence. In this new model turbulence governs the interaction between relativistic particles and magnetic field lines that diffuse, reconnect and are stretched in the turbulent ICM.

Key words: acceleration of particles - turbulence - magnetic reconnection - radiation mechanisms: non–thermal - galaxies: clusters: general

1 INTRODUCTION

Magnetic reconnection is a long-standing problem in astrophysics and plasma physics.

The traditional Sweet-Parker model of reconnection (Parker, 1957; Sweet, 1958) is very slow in all the astrophysical settings, which induced to searches of faster reconnection schemes. Petschek (1964) or X point reconnection for years has been the major contender for the mechanism for fast astrophysical reconnection. With plasma effects, e.g. Hall effect, included, the Petschek scheme looked promising to many researchers in the field (eg. Shay et al 1998, Birn et al 2001, Bhattacharjee 2004).

In parallel a scheme that invokes 3D Alfvenic turbulence was suggested in Lazarian & Vishniac (1999, henceforth LV99). The process appealed to MHD turbulence properties and predicted the independence of the reconnection rates on microphysics. Numerical simulations with externally induced turbulence supported analytical predictions in LV99 (eg. Kowal et al. 2011, 2012).

More recently, the Petschek scheme evolved into tearing reconnection, which presents much more chaotic state of the magnetic field evolution (Loureiro et al 2007, Uzdensky et al. 2010). Numerical simulations of tearing reconnection show a transition to turbulent state, although the role of turbulence for the reconnection in these simulations is debated (e.g., Karimabadi & Lazarian 2013 for review). Other simulations are suggestive of fast, i.e. independent of resistivity, magnetic reconnection even in the case when turbulence is not induced externally, but is generated by reconnection itself (Beresnyak 2013, Oishi et al. 2015, Lazarian et al. 2015).

These two schemes, the turbulent and tearing one, present at the moment two competing reconnection processes, which, as we discuss further in the paper, can be complementary and synergetic. In view of large-scale turbulence being present in the intra-cluster medium (ICM) (e.g., Brunetti & Jones 2014 (henceforth BJ14), Brueggen & Vazza 2015 for reviews), within this paper we mostly focus on the turbulent magnetic reconnection scheme.

The main aim of this paper is to explore a scenario of particle acceleration in the ICM where relativistic electrons are reaccelerated by the combined effect of super-Alfvenic turbulence and magnetic reconnection. As already mentioned turbulence and magnetic reconnection are interconnected aspects and reconnection can be fast in the presence of turbulence (LV99, Lazarian et al 2015 for review). In the presence of super-Alfvenic turbulence relativistic particles can diffuse across a complex network of regions of reconnection and magnetic field dynamo, where they are systematically accelerated or decelerated. This situation can be described as a combination of a first-order Fermi acceleration and a second order Fermi acceleration due to spatial random-walk across accelerating and decelerating regions. Under the assumption of *fast* diffusion from reconnection regions this chain of mechanisms becomes a second-order acceleration process and is the main focus of this paper.

Galaxy clusters are potential sites for this mechanism because super-Alfvenic turbulence is generated in the ICM. Evidence for relativistic electrons and magnetic fields in the ICM is routinely obtained from a variety of radio observations that detect diffuse synchrotron radiation from the ICM in the form of radio halos and relics (Feretti et al 2012, BJ14 for reviews). Giant radio halos and relics are found in disturbed clusters, suggesting that large scale motions that are generated during mergers provide the energy reservoir for the mechanisms of *in situ* particle acceleration (BJ14 for review on acceleration mechanisms in the ICM).

A popular scenario for the origin of radio halos is based on reacceleration induced by merger-driven turbulence (Brunetti et al 2001, Petrosian 2001, Fujita et al. 2003, Brunetti et al. 2004, BJ14 for review). In this model it is usually assumed that large-scale compressive turbulence generated during cluster mergers is transported at smaller scales via turbulent cascade and reaccelerates seed electrons (Cassano & Brunetti 2005, Brunetti & Lazarian 2007). This scenario has the potential to explain the observed properties of radio halos and it naturally explains their connection with mergers, still several challenges exist. Primarily the challenge is to determine the efficiency of particle acceleration that depends on the complex hierarchy of mechanisms that transport energy from large scale motions to collisionless particle-wave interactions at small-scales in the ICM (eg. Brunetti 2016 for a recent discussion). An additional challenge is that turbulent acceleration in the ICM is a slow process that cannot accelerate particles directly from the thermal pool (eg. Petrosian & East 2008). For this reason turbulent acceleration models require a population of seed electrons that are already ultra-relativistic (e.g., $\gamma \geq 100$) and that are spatially distributed on cluster scales (eg. Brunetti et al 2001, Brunetti & Lazarian 2011a, Pinzke et al 2015).

More recently numerical (fluid) simulations suggested that the compressive part of turbulence in the ICM is partially dissipated into weak shocks (see Miniati 2015, Porter et al 2015), implying that less energy is available for the mechanisms that are generally invoked in turbulent reacceleration models.

In order to overcome this last challenge we exploit our mechanism that is based on incompressible turbulence. We show that this mechanism may play a role in the reacceleration of relativistic electrons in the ICM under reasonable assumptions on the effective particle mean-free path.

In Sect.2 we discuss turbulent reconnection in super-Alfvenic turbulence. In Sect.3 we explain the acceleration mechanism and in Sect.4 we apply it to the case of cluster-scale radio emission in galaxy clusters. In Sect.5 we provide a discussion on CRs acceleration in the ICM and on the comparison between our model and other turbulent reacceleration models. We summarize results in Sect.6.

2 TURBULENCE AND MAGNETIC RECONNECTION

The ICM is a *weakly collisional* high-beta plasma and is expected to be turbulent at some level (BJ14, Bruggen & Vazza 2015 for reviews), the presence of instabilities in this plasma would make turbulence similar to MHD one (Santos-Lima et al 2015 and references therein). Natural drivers of ICM turbulence are the motions gravitationally driven by dark matter substructures that are generated in the ICM as a consequence of the hierarchical process of formation of galaxy clusters. As a consequence of these motions super-Alfvenic and sub-sonic turbulence should be driven in the ICM, although the way this turbulence is transported from large scale to small scale depends on details of ICM microphysics that are still poorly understood. It is believed that a hierarchy of processes in the ICM convert turbulent energy into non-linear amplification of magnetic fields, and particle heating and acceleration (eg. Ryu et al 2008, BJ14, Miniati & Beresnyak 2015).

Magnetic reconnection and dynamo are part of the turbulent cascade (eg. Lalescu et al 2015) and play a role in this complex hierarchy of mechanisms. Specifically, the model of turbulent reconnection by LV99 provides a natural extension of the classical Sweet-Parker model in the presence of turbulent motions.

Macroscopically the reconnection speed is constrained by the possibility to eject the plasma from the reconnection layer. It gives a maximum reconnection speed on macroscopic scales :

$$V_{rec} \approx V_A \frac{\Delta}{l_X} \tag{1}$$

where Δ is the thickness of the reconnection region (current sheet) and l_X is the astrophysical scale of the inflow associated with a reconnection region. In the classical Sweet-Parker model two regions with uniform *laminar* magnetic fields are separated by a thin current sheet, which is determined by microscopic resistivity. Over the thickness of this thin current sheet, Δ, the resistivity is important and the magnetic fields reconnect. However in astrophysical situations the disparity of scales between the inflow, l_X, and the outflow, Δ, strongly limit the reconnection rate (from Eq.1), implying $V_{rec} \ll V_A$.

One possibility to overcome this bottleneck is turbulence. Turbulence changes the direction of magnetic field lines that are subject to turbulent diffusivity. Under these conditions the outflow Δ gets much thicker, being determined not by microphysics of resistivity, but by macroscopic field wandering in 3D (LV99). LV99 derived the reconnection rate for sub-Alfvenic turbulence, this is $V_{rec} \sim (l_X/L_o)^{1/2} M_A^2 V_A$,

where L_o and M_A are the turbulent injection scale and Alfven Mach number, respectively.
Results can be easily extended into the super-Alfvenic regime (Lazarian et al 2015) that is typical of the ICM. An intuitive way to estimate Δ in super-Alfvenic turbulence is to use the diffusion properties of magnetic field lines. In this approach Δ is essentially the diffusion scale covered by magnetic field lines within the time-period necessary to expel the plasma from the reconnection region, $\tau_A \sim l_X/V_A$. It has been shown that field diffusion in these conditions is similar to Richardson diffusion in hydro- motions (Eyink et al 2013). It implies $\Delta^2 \approx \epsilon\tau_A^3$, where $\epsilon \sim \delta V^3/L_o$ is the specific turbulent energy rate, from which one immediately gets $\Delta \sim l_A$.
The other ingredient to determine a macroscopic constraint to the reconnection speed in Eq.1 is the inflow, astrophysical, scale of reconnection regions l_X. Super-Alfvenic turbulence naturally generates regions of magnetic field reversals everywhere in the plasma with minimum scale of the order of the MHD scale $l_A = L_o M_A^{-3}$. At scales $l > l_A$ kinetic energy is in excess of magnetic energy inducing a continuous change of magnetic field topology, due to advection of field lines by hydro- motions, and consequently quenching the reconnection process. Under these conditions the dominant scale for the inflow in reconnection regions is expected to be $l_X \sim l_A$. As a consequence we may think of a situation of *fat* reconnection regions in super-Alfvenic turbulence, with $\Delta \sim l_X \sim l_A$, where the macroscopic reconnection speed can approach the Alfven speed (Eq.1).
In the following we shall adopt this configuration to calculate particle acceleration.

3 ACCELERATION OF RELATIVISTIC PARTICLES IN RECONNECTION

3.1 Brief Overview on acceleration in turbulent reconnection

Particle acceleration in reconnection regions has been investigated in different environments and considering different mechanisms (e.g., Lyutikov & Blandford 2003, Lyubarsky 2003, Drake et al 2006, 2010, 2013, Lazarian & Opher 2009, Lazarian & Desiati 2010, Kowal et al 2011, Giannios 2013, Sironi & Spitkovsky 2014, Zank et al 2014).
One mechanism has been proposed within turbulent reconnecting regions. Turbulent reconnection results in shrinking of 3D magnetic bundles and the charged particles entrained over magnetic loops can be accelerated by firts-order Fermi mechanism (de Gouveia dal Pino & Lazarian 2005). This mechanism has been used to model particle acceleration in several environments, including gamma-ray bursts (Zhang & Yan 2011), low luminosity AGNs (Kadowaki et al 2015), microquasars (Khiali et al 2015) and in the heliosphere (Lazarian & Desiati 2010). Interestingly, the compressibility is not necessary in this mechanism *. The physics of the acceleration is easy to understand. Magnetic reconnection induces systematic shrinking of magnetic field lines on scales $\leq l_A$ and particles entrained on these field lines are getting energy as the consequence of the Liouville theorem.
Particle acceleration in turbulent reconnection sites has also been investigated by numerical studies that combine MHD simulations and tracer particles (eg., Kowal et al 2011,12). The acceleration of particles trapped within converging reconnection regions is consistent with first-order Fermi mechanisms.
In a general situation presumably particles interact with multiple reconnection layers and turbulence experiencing a hierarchy of processes at different scales and energies. An exploratory investigation of this situation is the main focus of this Section (Sect.3.2). However we anticipate that the basic picture deriving from our study does not depend critically on the specific mechanism of particle acceleration within reconnecting regions (see Sect.3.3).

3.2 Our approach

Here we follow a simple approach to explore the general situation where relativistic particles are reaccelerated diffusing on large-scale super-Alfvenic turbulence and reconnection regions. We proceed with the following assumptions:

i) large-scale turbulence in the ICM behaves collisional and MHD provides a good guide as far as reconnection is considered;
ii) ultra-relativistic CRe are collisionless components interacting with fluctuations in the MHD fluid;
iii) we assume a scenario based on turbulent reconnection, where diffusion of magnetic field lines governs the process of scattering of CRs;
iv) we expressly investigate only the collisionless effects that involve the interactions between large-scale magnetic field lines and CRe.

It is difficult to establish to what extent these assumptions allow a solid description of the ICM. The main point here is that we need reconnection events in terms of (belonging to) MHD cascade. However it is worth to note that even if turbulence in the ICM is collisionless we may still expect that the dynamics of the magnetic field lines can be described according to Alfvenic turbulence (Eyink et al 2011, Makwana et al 2015), thus supporting our basic assumptions.

We start considering particles within reconnecting regions. The increment in momentum of particles after the interaction with shrinking magnetic field lines can be estimated as :

$$\Delta p \simeq \Delta t \times \frac{dp}{dt} \tag{2}$$

where the time-scale spent by particles in a reconnecting region is :

$$\Delta t = \min\left\{\frac{l_A}{V_A}, \frac{l_A^2}{D}\right\} \tag{3}$$

where $\frac{l_A}{V_A}$ is the turn-over time of eddies (corresponding to *slow* diffusion limit) and $\frac{l_A^2}{D}$ is the particle diffusion time on scale l_A (corresponding to *fast* diffusion, D is the spatial diffusion coefficient of CRe), and

$$\frac{dp}{dt} \sim \phi\frac{V_A}{\lambda_{mfp}}p \tag{4}$$

* a generalised version of the mechanism in the presence of compression is discussed in Drury (2012)

where λ_{mfp} is the particles mean free path (mfp) and $\phi \sim 1$ accounts for pitch angle distribution and geometry of scatterings.
However, in a turbulent fluid with stationary turbulence the reconnection process should be accompanied by the opposite process of magnetic field generation, i.e. by turbulent dynamo. Naturally, this process results in a stretching of the magnetic field lines that on scale l_A occurs on a timescale l_A/V_A and that *statistically* compensates field diffusion on the same scale (Beresnyak & Lazarian 2015). It results in a situation where energetic particles within dynamo regions cool by an amount that is similar (in absolute value) to that of the acceleration in reconnection regions.
Therefore if particles can diffuse across these regions, we expect that they will undergo cycles of first order acceleration in reconnection regions and cycles of cooling in dynamo regions. This is the theoretical picture that we use to describe the acceleration of particles diffusing in a turbulent fluid on scales larger than l_A. It differs from the traditional second order Fermi acceleration because the increments of the momentum of the CR in the acceleration and deceleration regions in principle can be comparable with the momentum of the CR.

In order to estimate the acceleration rate resulting from this complex mechanism we make the educated guess that reconnecting and dynamo regions are statistically distributed everywhere in the astrophysical volume on typical scales $\sim l_A$. This can be motivated by the fact that the generation of magnetic fields and field reconnection occur indeed everywhere in the volume, although this assumption needs to be evaluated more carefully in follow up studies.
For $\Delta p \ll p$ in Eq.2, particles interacting with these regions will undergo a random-walk process in the momentum space resembling a second-order Fermi mechanism. From Eqs.2–4 this condition implies $\lambda_{mfp} \gg \phi l_A$ (in the slow diffusion) or $\lambda_{mfp} > l_A(3\phi V_A/c)^{1/2}$ (*fast* diffusion, assuming $D \sim \frac{1}{3}c\lambda_{mfp}$). This also tells us that the condition $\Delta p \ll p$ in the ICM is possible only in the case of *fast* diffusion, because *slow* diffusion (Eq. 3) occurs for $\lambda_{mfp} \leq 3V_A l_A/c \ll l_A$.

In the following we will restrict to the case of fast diffusion and to situations where $\Delta p \ll p$. Under these conditions particles undergo a diffusion process in the momentum space and retain a isotropic distribution of pitch angles, provided that the pitch-angle scattering rate, $\tau_{sc} \sim \lambda_{mfp}/c$, is fast enough. The distribution function of particles in the momentum space, $f(p)$, evolves according to a isotropic Fokker-Planck equation (e.g., Schlickeiser 2002):

$$\frac{\partial f(p,t)}{\partial t} = \frac{1}{p^2}\frac{\partial}{\partial p}\left(p^2 D_{pp}\frac{\partial f}{\partial p} - p^2 \sum \left|\frac{dp}{dt}\right|_{loss} f(p,t)\right) + Q(p,t) - \frac{f(p,t)}{T_{esc}} \quad (5)$$

where the diffusion coefficient in the particle momentum space is (Eqs.2–4) :

$$D_{pp} = \langle \frac{\Delta p \Delta p}{2\Delta t} \rangle \sim 3\left(\frac{l_A}{\lambda_{mfp}}\right)^2 \frac{V_A^2}{\lambda_{mfp} c} p^2 \quad (6)$$

implying a reacceleration time $\tau_{acc} \sim p^2/(4D_{pp})$, and where $\sum \left|\frac{dp}{dt}\right|_{loss}$ accounts for the energy losses in the ICM (synchrotron, ICS, Coulomb, ..), Q accounts for injection of new particles, and f/T_{esc} accounts for diffusion/escape of particles from the region (T_{esc} is the escaping time).
Solutions of Eq.5 in the case $D_{pp} \propto p^2$ are calculated in numerous papers (eg Schlickeiser 1984, Mertsch 2011, for numerical solutions Donnert & Brunetti 2014 and references therein). We anticipated that $D_{pp} \propto p^2$ also results from reacceleration by compressible turbulence (both Transit-Time-Damping and stochastic compressions) in the ICM and consequently the properties of the spectra of reaccelerated electrons expected in our model will be similar to those calculated in other studies (BL07, Brunetti & Lazarian 2011a, ZuHone et al 2013, Donnert & Brunetti 2014; see Sects. 4 and 5).

The acceleration rate from Eq.6 depends on the particles mfp that however is poorly known. In super-Alfvenic turbulence hydro- motions change directions of magnetic field lines on scales $\geq l_A$. This configuration automatically defines a maximum effective mfp of particles, $\lambda_{mfp} \sim l_A$, because particles travelling in tangled fields change directions on this scale preserving the adiabatic invariant. In addition magnetic field fluctuations in MHD turbulence induce particles pitch-angle scattering via resonant interaction and affect the motion of particles. This is different from the previous interaction because in this case particles experience pitch-angle scattering with respect to the local field direction and do not preserve adiabatic invariant. The parallel mfp from this process is :

$$\lambda_{mfp} = \frac{3c}{4}\int_0^1 d\mu \frac{\left(1-\mu^2\right)^2}{D_{\mu\mu}} \quad (7)$$

where $D_{\mu\mu}$ is the pitch-angle diffusion coefficient. In the case of incompressible MHD turbulence on scales $< l_A$ resonant pitch-angle scattering is dominated by transit-time-damping with pseudo-Alfven modes (Yan & Lazarian 2008, Beresnyak et al 2011). In the super-Alfvenic case the interaction is dominated by the largest moving mirrors with $l \sim l_A$, and from Eqs 8-9 in Yan & Lazarian (2008) (in the limit $M_A \to 1$ and $L \to l_A$) we find $D_{\mu\mu} \sim \frac{c}{l_A}F(\mu)$, where $F(\mu) \sim 1$ for transverse propagation and $F \ll 1$ in the quasi-parallel case. In this case Eq.7 gives $\lambda_{mfp} \sim l_A$.
In conclusion particles interacting with large-scale incompressible and super-Alfvenic MHD turbulence will change direction on time scales $\sim l_A/c$ due to magnetic field tangling and at the same time will experience pitch-angle scattering on time scale $\sim F(\mu)^{-1} l_A/c$. It basically implies an average effective mfp that is a fraction of l_A, $\lambda_{mfp} = \psi l_A$, where $\psi < 1$; additional mechanisms of pitch-angle scattering from kinetic/plasma effects will further reduce λ_{mfp} (Sect. 3.3).
It is thus convenient to re-write relevant quantities in terms of $\beta_{pl} = 2\Gamma^{-1}c_s^2/V_A^2$ ($\Gamma = 5/3$) and the particles mfp in terms of the Alfvén scale, l_A :

$$D_{pp} \simeq 3\sqrt{\frac{5}{6}}\frac{c_s^2}{c}\frac{\sqrt{\beta_{pl}}}{L_o} M_t^3 \psi^{-3} p^2 \quad (8)$$

and

$$l_A = L_o M_A^{-3} = \frac{(6/5)^{3/2} L_o}{(\sqrt{\beta_{pl}} M_t)^3} \quad (9)$$

Note that the condition $\Delta p \ll p$ is satisfied for:

$$\psi > \sqrt{\frac{(3c_s\sqrt{6/5})}{(c\sqrt{\beta_{pl}})}} \quad (10)$$

3.3 A note on the role of kinetic effects

The role of kinetic effects on small scales is different for the turbulent reconnection (see LV99, Kowal et al. 2009, Eyink et al. 2011, 2013, Eyink 2015, Lazarian et al. 2015) and tearing reconnection (see Loureiro et al. 2007, Uzdensky et al. 2010, Ng et al. 2015). Kinetic effects in the latter process accelerate the reconnection rate inducing tearing of the current sheet. On the contrary, turbulent reconnection is independent of the detailed kinetic physics, as follows from theory (LV99, Eyink 2015) and confirmed in numerical simulations where plasma physics effects were introduced using anomalous resistivity (see Kowal et al. 2009). Both approaches can be complementary with tearing destabilizing the reconnection sheet if the level of turbulence in the system is low. The outflow from the reconnection layer for extended current sheets has the thickness Δ and the *Reynolds* number $Re \sim V_A\Delta/\nu$, where ν is viscosity, which for the ICM should be taken the perpendicular Braginsky viscosity. With tearing inducing $V_{rec} > 0.01V_A$, which in turn is of the order of $V_A\Delta/l_x$ (eq.1), Δ gets to be $> 0.01\, l_x$, making the *Reynolds* numbers of the outflow sufficiently large. This should make the outflow turbulent and is likely to transfer the reconnection into a regime similar to turbulent reconnection.

The physics of acceleration in turbulent and tearing reconnection in 3D is very similar. The difference initially were due to the fact that acceleration in turbulent reconnection was considered in 3D (de Gouveia dal Pino & Lazarian 2005) while acceleration in tearing was considered in 2D (Drake et al 2006). As the actual 3D geometry of astrophysical reconnection is being acknowledged and tearing reconnection layers demonstrate more turbulence as the numerical resolution increases, strong similarities emerge between the two mechanisms with the acceleration being essentially related to the shrinking of 3D loops[†].

It is also true that particle acceleration and transport in reconnection regions are potentially sensitive to details of the physics of reconnection (eg., Daughton et al 2011). More recently the controversy on whether the tearing reconnection is second or first order has emerged. For example Drake et al (2013) find a shortening of magnetic island field line length because of adjacent islands merging. This causes an increase in the parallel particle velocity and a decrease in perpendicular energy suggesting second order rather than first order Fermi mechanisms. In fact attempts to model second order Fermi acceleration of particles diffusing across multiple reconnecting regions have been developed in the case of collisionless tearing reconnection mediated by quasi 2D magnetic islands (eg. Le Roux et al 2015).

In Sect.3.2 we have assumed first order acceleration in reconnection regions because this mechanism has been clearly demonstrated in numerical simulations of turbulent reconnection (Kowal et al 2012). We would believe that a similar effect should be present also in tearing reconnection. While the relative importance of the second and first order Fermi acceleration in tearing reconnection may need to be settled in future, for our treatment of the acceleration this is not so vital and in principle our picture can be extended also to the case of tearing reconnection. In fact, we only require that a particle leaving the reconnection region gained the momentum Δp whatever is the cause of the acceleration [‡]. Once CRe leave reconnecting regions they will interact with the dynamics of magnetic field lines on very large scales, $l_A \sim$ 100 pc – kpc. On these large scales reconnection events are part of the turbulent cascade and we can use transport properties that follow from MHD turbulence (Sect. 3.2).

The microphysics of the plasma may still be important for particle acceleration and reacceleration even if the reconnection rates are determined by the LV99 mechanism. In fact kinetic/plasma effects on small scales may induce pitch-angle scattering events in addition to those due to the MHD fluctuations on large scales considered in Sect.3.2. Overall the combined effects of scatterings on small and large scales can be parameterized in the form of the particles mfp, λ_{mfp}, and in general scatterings on small scales are expected to reduce λ_{mfp} with respect to that in Sect.3.2 and increase the acceleration rate. We note that the small-scale physics is likely to be important when we consider the acceleration of particles from the thermal pool. In this rescpect, potentially kinetic/plasma effects might provide also a solution to the problem of *seed* particles in reacceleration models (Sect.1), however we do not address the issue of the acceleration of energetic particles from the thermal pool in this paper.

4 DIFFUSE RADIO EMISSION IN GALAXY CLUSTERS

4.1 Current view

Turbulence and shocks are generally invoked to play a role for the origin of radio halos and radio relics in galaxy clusters (BJ14 for review). Nevertheless recent observations of the radio relic in A2256 unveiled a complex/filamentary morphology of the radio emission and no clear evidence for a direct connection with a shock, hinting a possible role of magnetic reconnection (Owen et al 2014). A role of magnetic reconnection for the origin of non-thermal components in galaxy clusters was also envisaged on theoretical grounds by Lazarian & Brunetti (2011).

Radio halos are the most prominent non-thermal sources in galaxy clusters. A popular scenario for their origin is based on the hypothesis that turbulence generated during cluster mergers (re)accelerates seeds electrons on Mpc scales (Brunetti et al 2001, Petrosian 2001, BJ14 for review). Crucial ingredients of this scenario are however poorly known. Primarily the challenge is to understand the chain of mechanisms that allow to drain energy from large scale motions into mechanisms acting on smaller scales and that in turn

[†] a comparison of particle acceleration rates in 2D and 3D configurations is discussed in Kowal et al. (2011)

[‡] In the case of second order acceleration the term dp/dt in our eq.4 can be seen as the *systematic* part of a second order process occurring within reconnection regions, i.e. $dp/dt \sim \tilde{D}_{pp}/4p$ where $\tilde{D}_{pp}$ is the diffusion coefficient in the particles' momentum space due to such a hypothetical second-order mechanism on smaller scales

determines the efficiency of acceleration (see Brunetti 2016 for a recent discussion).
Presumably several turbulent components are generated in the ICM, both at large and very small scales,and all these components should jointly contribute to the scattering and (re)acceleration of relativistic particles. In the last years much attention has been devoted to the role of compressible turbulence that is driven at large scales in the ICM from cluster mergers and that cascades at smaller scales (Cassano & Brunetti 2005, Brunetti & Lazarian 2007, 2011a). This is the simplest scenario that can be thought, nevertheless it predicts a straightforward connection between cluster mergers and radio halos in agreement with observations. This is also the scenario adopted in follow-up numerical simulations that aim at investigating the origin of diffuse radio emission in galaxy clusters (Donnert et al 2013, Beresnyak et al 2013, Donnert & Brunetti 2014, Miniati 2015, Pinzke et al 2015).

On the other hand, recent numerical simulations of cluster formation have shown that most of the turbulence in galaxy clusters is solenoidal (see Miniati 2015). Although these simulations show that compressive turbulence is also generated in connection with clusters mergers, this component is found fairly short living (≤Gyr) and with a kinetic spectrum that is steeper than that previously assumed in calculations of turbulent acceleration. The consequence is a reduction of both the reacceleration period and the acceleration rate. In reality these simulations do not tell us much about the microphysics (eg. particles collision frequency) and power spectrum of electromagnetic fluctuations that both govern the acceleration efficiency and *di per se* do not challenge acceleration models based on compressive turbulence generated at large-scale (Miniati 2015, Brunetti 2016). However these are clearly thought-provoking results that motivate us to investigate possible mechanisms that drain a fraction of the solenoidal turbulence in the ICM into particle acceleration.

4.2 A new mechanism ?

In this respect the mechanism described in Sect.3 is particularly attractive as it is based on super-Alfvenic solenoidal turbulence. If we restrict to the situation of *fast* diffusion regime, the acceleration time is (Eq.8) :

$$\tau_{acc} = \frac{p^2}{4D_{pp}} \simeq \frac{\sqrt{6/5}}{12}\frac{c}{c_s^2}\frac{L_o}{\sqrt{\beta_{pl}}}M_t^{-3}\psi^3 \qquad (11)$$

and the acceleration rate (or efficiency, throughout this paper) $= \tau_{acc}^{-1}$. The acceleration time is reported in Fig.1 as a function of the CRe mfp, $\psi = \lambda_{mfp}/l_A$, assuming typical conditions in the ICM; the acceleration efficiency rapidly increases with decreasing CRe mfp. Fig.2 shows the effect induced on the acceleration time by increasing the turbulent Mach number and β_{pl}: for given values of ψ and of the turbulent injection scale, L_o, the acceleration rate increases with both Mach number and β_{pl}. Calculations in Fig.2 are obtained for typical conditions in the ICM, specifically we assume a range of $\beta_{pl} \sim 30 - 120$ that is inferred using values of magnetic field derived from Faraday rotation measures (eg., Carilli & Taylor 2002, Feretti et al 2012) and turbulent injection scales $L_o \geq 100$ kpc (BJ14, Brüggen & Vazza 2015).

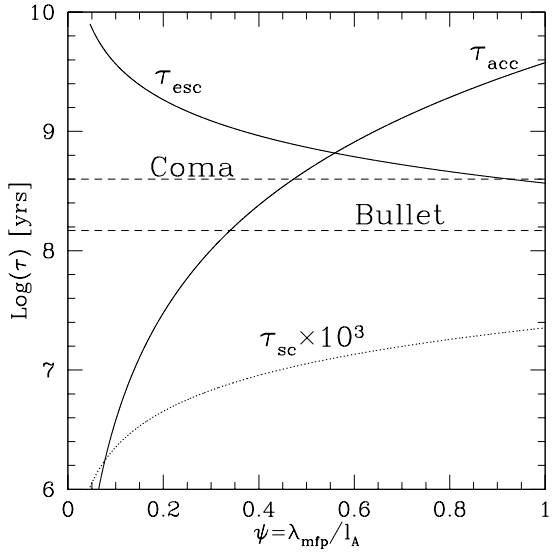

Figure 1. Acceleration time-scales as a function of ψ. Horizontal dashed lines are the maximum reacceleration times, τ_{max}, requested for the radio halos in the Coma and Bullet clusters (Eq.14, see text). Diffusion time on $L_{RH} = 1$ Mpc (eq.12) and scattering time-scale, λ_{mfp}/c (multiplied by 1000 for display proposal), are also reported. Calculations are obtained assuming $M_t^2 = 0.25$, $L_o = 300$ kpc, $\beta_{pl} = 60$, $c_s = 1500$ km/s.

In our model the mfp is a free parameter that is difficult to calculate from first principles due to our ignorance of kinetic effects on small scales (see Sect.3 for constraints based on MHD and 3.3 for a discussion on kinetic effects). However we can also infer independent constraints on that. Statistics of radio halos suggests that they are generated in massive mergers for a significant fraction of the duration of these events (eg., Brunetti et al 2009, Cassano et al 2013, Cuciti et al 2015). It implies that CRe should be trapped within the emitting, Mpc-scale, volume for ≥ few Gyr. This provides a limit to the diffusion time of CRe on these scales and thus on their maximum mfp. The time needed by CRe to diffuse on the scale of a radio halo, L_{RH}, is :

$$\tau_{esc} \sim \frac{L_{RH}^2}{4D} \sim \frac{5}{8}\sqrt{\frac{5}{6}}\frac{1}{c}\left(\sqrt{\beta_{pl}}M_t\right)^3\frac{L_{RH}^2}{L_o}\psi^{-1} \qquad (12)$$

that is reported in Fig.1. The minimal condition $\tau_{esc} \geq$ few Gyrs implies $\lambda_{mfp} \ll$ kpc, or in terms of MHD scale, $\psi < 0.5(\beta_{pl}/60)^{\frac{3}{2}}(M_t/0.5)^3(L_o/300\text{kpc})^{-1}$ (Fig.1, Eq.12), i.e. larger values of the turbulent Mach number and of the β_{pl} constrain larger values of ψ. We note that the ratio of acceleration and diffusion time, $\tau_{acc}/\tau_{esc} \propto \psi^4 L_o^2 M_t^{-6}$, rapidly decreases with increasing the turbulent Mach number for a given value of ψ and of the injection scale L_o (Fig.2).
Finally, we note that very small values of the mfp, that imply faster acceleration (Eq.11), are also ruled out from the condition $\Delta p \ll p$ (Eq.10).

Given these constraints on λ_{mfp} and ψ, the following point is to understand whether our mechanism can explain the diffuse radio emission observed in galaxy clusters. To fully address this point Fokker-Planck time-dependent calculations are necessary (Eq.5). However, as we anticipated

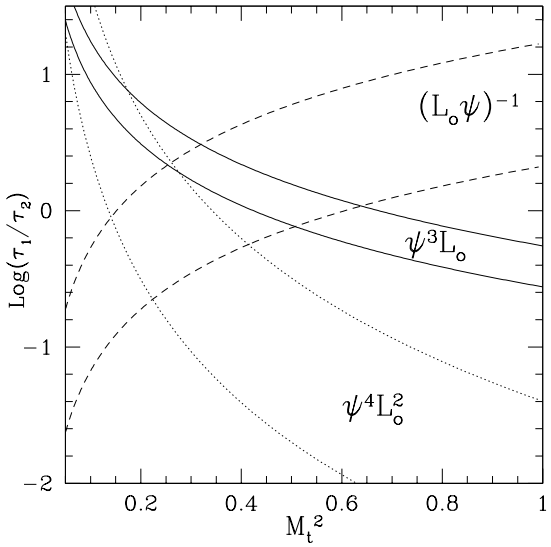

Figure 2. Ratio of model acceleration time and the τ_{max} =150 Myrs for the Bullet radio halo (solid lines), and ratio of model acceleration time and diffusion time on 1 Mpc (dotted lines) as a function of the turbulent Mach number. Calculations assume a reference value $\psi = 0.5$, and β_{pl} =30 and 120 (from top to bottom); other parameters being equal to Fig.1. Dashed lines are the diffusion times in Gyr (from top to bottom with decreasing β_{pl}). Dependences on ψ and L_o are shown in the panels.

in Sect.3.2, numerous papers carry out Fokker-Planck calculations of particle reacceleration in galaxy clusters in the case $D_{pp} \propto p^2$. These results can be automatically extended to our model and for this reason in this exploratory paper we do not focus on Fokker-Planck analysis.

In practice two main processes oppose to the reacceleration of CRe.

Synchrotron and inverse Compton losses balance the acceleration of CRe channelling an increasing fraction of the energy gained by CRe into radiation. The time-scale of radiative losses (radiative life-time) of CRe is :

$$\tau_{rad}(\gamma) = \gamma / \frac{d\gamma}{dt} = \frac{6\pi m_e c}{\sigma_T} \frac{\gamma^{-1}}{B^2 + B_{cmb}^2} \quad (13)$$

where $B_{cmb} \simeq 3.25(1+z)^2 \mu$G is the equivalent field due to inverse Compton scattering with photons of the Cosmic Microwave Background. In the ICM the CRe that produce synchrotron radiation in the radio band have energies $\sim$ few GeV and radiative life-times $\tau_{rad} \sim 100$ Myrs (BJ14 for review). The acceleration mechanisms that generate steep spectrum radio emission in galaxy clusters should have an efficiency that is comparable to that of the radiative losses of the CRe that emit the observed radio emission. Consequently, due to the balance between acceleration and losses, after a reacceleration period of about 100 Myrs the spectrum of radio emitting CRe evolves slowly with time and approaches quasi-stationary conditions, provided that the acceleration rate is constant (BJ14 for review and references therein).

The second process that opposes to reacceleration is more subtle and is due to physical mechanisms that may damp the turbulent spectrum reducing with time the energy flux that becomes available for the reacceleration of CRs. In this respect the most obvious process is the damping (via collisionless dampings) of turbulence due to the same CRs that are reaccelerated. This mechanism may affect (reduce) the acceleration rate on longer timescales (BJ14 for review and references therein).

In this Section we consider only the first damping mechanism, due to radiative losses of CRe, whereas in Sect.5.2 we will discuss the turbulence damping.

In practice, the most relevant point here is to check whether our mechanism allows reacceleration of CRe to the energies that are necessary to produce the synchrotron radiation observed in galaxy clusters. In Figs.1 and 2 the acceleration time is compared with the acceleration time that is requested for radio halos. This is not necessarily equivalent to the radiative cooling time of the CRe emitting at the observed radio frequencies, because radio halos have very steep synchrotron spectra, $\alpha \sim 1-2$ (flux $\propto \nu^{-\alpha}$). In this respect we use results from Cassano et al.(2010) that calculated synchrotron spectra in homogeneous models of compressive turbulent reacceleration (with $D_{pp} \propto p^2$) assuming reacceleration periods in the range $\Delta t/\tau_{acc} \sim 2-4$. They found that the spectra become steeper than those of typical radio halos at frequencies greater than $\nu_s \sim \xi\nu_b$, where $\xi \sim 6-8$, and ν_b is the critical synchrotron frequency emitted by electrons having acceleration time equal to the time-scale of radiative losses, i.e. CRe with Lorentz factor $\gamma_b = \frac{6\pi m_e c}{\sigma_T} \tau_{acc}^{-1}/(B^2 + B_{cmb}^2)$. The highest frequency is generated in a magnetic field $B \sim B_{cmb}/\sqrt{3}$, since this is the field where CRe emitting at a given frequency have maximum lifetime. It leads to a *minimal* request for a mechanism being sufficient to reaccelerate CRe emitting at the observed frequency $\nu_o = \nu_s/(1+z)$. This condition corresponds to a *maximum* reacceleration time, τ_{max} :

$$\tau_{acc} \leq \tau_{max} = 156 \left(\frac{\xi}{\nu_o(GHz)}\right)^{\frac{1}{2}} (1+z)^{-7/2} \quad \text{(Myr)} \quad (14)$$

In Figs.1 and 2 we report relevant values of τ_{max} derived from Eq.14. These values are derived for the radio halos in the Coma and Bullet clusters, $\tau_{max} = 400$ and $= 150$ Myr, respectively, by considering observed steepening frequencies $\nu_o \simeq 1$ GHz for Coma (eg. Brunetti et al 2013 and references therein) and $\simeq 5$ GHz for the Bullet cluster (a hint of steepening is observed in this cluster at ~ 8 GHz, Liang et al 2000, Shimwell et al 2014, Marchegiani & Colafrancesco 2015).

The comparison between τ_{max} and the reacceleration time predicted by our model selects the parameters space (M_t, ψ, L_o) that allows to explain radio halos. Specifically, the acceleration time predicted by our model (Eq.11) leads to a steepening frequency :

$$\nu_s(\text{GHz}) \simeq 2.45 \left(\frac{c_s}{10^3 \frac{\text{km}}{\text{s}}}\right)^4 \frac{\beta_{pl}}{10^2} \frac{\xi}{7} \left(\frac{10^2 \text{kpc}}{L_o}\right)^2 \left(\frac{M_t}{0.5} \frac{0.5}{\psi}\right)^6 \times \left(\frac{B_{\mu G}}{(B_{\mu G}^2 + B_{cmb}^2)^2}\right) / 0.01 \quad (15)$$

implying that an emitting synchrotron frequency 10 times larger is produced by increasing the turbulent Mach number

(or reducing the CRe mfp) by about 50 percent, or by assuming a turbulent-injection scale that is 3 times smaller. For $B \simeq B_{cmb}/\sqrt{3}$, the Mach number and the observed steepening frequency in our model are connected via (from Eq.15) :

$$M_t \simeq 0.8 \frac{10^3 \frac{\rm km}{\rm s}}{c_s} \left(\frac{\nu_o({\rm GHz})}{35} \frac{7}{\xi} \right)^{\frac{1}{6}} \left(\frac{L_o}{10^2 {\rm kpc}} \right)^{\frac{1}{3}} \frac{(1+z)^{\frac{7}{6}} \frac{\psi}{0.5}}{(\frac{n_{ICM}}{10^{-3}})^{\frac{1}{6}}} \quad (16)$$

that allows us to conclude that turbulent Mach numbers $M_t^2 \sim 0.2{-}0.5(\psi/0.5)^2 (L_o/300\,{\rm kpc})^{2/3}$ are sufficient to reaccelerate CRe that generate synchrotron radio emission in hot, kT $\sim 5-15$ keV, clusters. Note that under these conditions the model satisfies also the additional requirements that are necessary to explain radio halos and cluster-scale radio emission, specifically the acceleration time is shorter than the diffusion time of CRe ($\tau_{acc} < \tau_{esc}$) and CRe are efficiently trapped within Mpc-scale emitting regions, i.e. $\tau_{esc} >$ few Gyrs (Figs.1 and 2). We note that the above amount of turbulent energy/Mach numbers is consistent with that found in high-resolution cosmological (fluid) simulations (eg., Vazza et al 2011, Miniati 2015).
Interestingly the same turbulent motions that are used in our model to reaccelerate particles will induce a broadening of the X-ray lines (for example the FeXXV lines at 6.7 keV) that can be tested by the forthcoming ASTRO-H satellite (Kitayama et al 2014) and, in the not too distant future, by ATHENA (Ettori et al. 2013). In particular, assuming a typical electron number density $= 10^{-3}{\rm cm}^{-3}$, from Eq.16 we get *minimum* turbulent velocities at the scale L_o, $\delta V_o \sim 700$ and $450(\psi/0.5)(L_o/100{\rm kpc})^{1/3}$ km/s for the halo in the Bullet and Coma clusters, respectively (corresponding to Mach numbers $\simeq 0.35$ and 0.3, respectively) (see also Sect. 5).

At this point it is worth to comment that our conclusions are based on results from compressive turbulent acceleration models in the homogeneous case and on their scaling to our model. Follow up Fokker-Planck time-dependent calculations combined with numerical simulations are required to account for non-homogeneous distributions of the physical parameters in the turbulent ICM (see discussion in Sect. 4.3) and to model the time evolution of the synchrotron spectrum of cluster-scale emission. For example, with regard to this latter point, the parameter $\xi \sim 6-8$ in Eqs.14–16 is derived for acceleration periods $\Delta t/\tau_{acc} \sim 2-4$ (Cassano et al 2010) (i.e. $\Delta t \sim 0.3-1$ Gyr for typical values of τ_{acc}), corresponding to a situation where radio spectra evolve slowly with time (quasi-stationary) because reacceleration is balanced by the energy losses of the CRe emitting in the radio band. On the other hand the shape of the spectrum of radio halos may be different during earlier and/or later phases. During earlier phases reacceleration is not balanced yet by losses and the spectrum rapidly evolves with time being very steep (implying smaller ξ) at the beginning of the reacceleration phase ($\Delta t/\tau_{acc} < 2$). Similarly, at later stages the evolution of CRe spectrum is potentially affected by saturation effects due to turbulence damping (see Sect. 5).

4.3 A note on the spectrum of radio halos

The spectral shape of radio halos provides information that go beyond simple arguments based on acceleration timescales. Unfortunately due to observational limitations a spectrum with at least three measurements is available only for a few halos, and significant scatter of measurements is seen in the cases where the data-points cover at least 1 order of magnitude in frequency range (e.g. Macario et al 2013, Shimwell et al 2014). Current studies suggest that the spectra of radio halos are quite different. Assuming a simple power-law shape (in the form flux $\propto \nu^{-\alpha}$) the spectral slopes measured between two typical frequencies (0.3 – 1.4 GHz) are currently found in the range $\alpha \sim 1-2$ (eg Venturi 2011). The Coma radio halo is a unique case with several spectral measurements covering about 2 orders of magnitude in frequency. Despite the scatter that is observed between the different measurements a spectral steepening is observed at higher frequencies, suggesting a corresponding break in the spectrum of the emitting electrons (Brunetti et al 2013 and references therein).

We still lack a comprehensive understanding of the spectrum of radio halos predicted in reacceleration models. In the context of our model and in the other turbulent reacceleration models, the spectrum of radio halos results from the interplay between the CRe spectrum and the probability distribution function (PDF) of magnetic field strengths in the emitting volume. Simple homogeneous reacceleration models, where both the magnetic field and acceleration rate are constant in the emitting volume, predict a curved spectrum due to the interplay between energy losses and diffusion in the particle's momentum space (e.g. Cassano & Brunetti 2005). More realistic turbulent models account (at least) for the decline of the magnetic field strength with radius in clusters. The effect is a stretching in frequency of the volume-integrated synchrotron spectrum of the halos that allows to successfully explain observed spectra (BL07, Brunetti et al 2008, Brunetti & Lazarian 2011a, Macario et al 2013, Donnert et al 2013). In the real case of a turbulent ICM the magnetic PDF is expected to be broad, and the turbulent and plasma-collisional properties can vary in the emitting, Mpc, volume. This, combined with the possibility of CRe diffusion across different turbulent regions, is expected to stretch considerably the synchrotron spectrum in frequency. Examples of synchrotron spectra from non-homogeneous turbulent reacceleration can be found in ZuHone et al (2013), where turbulent acceleration with $D_{pp} \propto p^2$ and synchrotron emission from mini-halos (cluster's core) are calculated using high-resolution (kpc) MHD simulations combined with tracer particles to follow the dynamics and evolution of CRe.

5 DISCUSSION ON CRS REACCELERATION IN THE ICM

5.1 A comparison with reacceleration by compressive turbulence

In this Section we compare our model with stochastic reacceleration models by compressible turbulence in the ICM.

We start from the the momentum-diffusion coefficient that is expected in the classical Fermi theory. This is (e.g., Longair 2011):

$$D_{pp} \sim p^2 \frac{\delta V_l^2}{cl} \sim p^2 \frac{V_{ph}^2}{cl} \frac{(\delta B)_l^2}{B_0^2} \quad (17)$$

where l is the minimum scale of eddies, V_{ph} is the phase

velocity of waves and in high-beta plasma conditions it is $\delta B/B_0 \sim \delta V/V_{ph}$. It follows that D_{pp}/p^2 is simply $c/\delta V_l$ times the turn-over time of turbulent eddies at the dissipation scale.

These dependences basically apply also to the case of the interaction between compressible turbulence (essentially fast modes) and particles via Transit-Time-Damping (TTD). TTD interacts through the $n = 0$ Landau resonance (eg. Fisk 1976, Schlickeiser & Miller 1998). This interaction is essentially the coupling between the magnetic moment of particles and the parallel magnetic field gradients and it uses the turbulent energy that is available on a broad range of scales, in principle between the dissipation and the injection scales. The diffusion coefficient in the particles momentum space due to TTD in the ICM is derived in BL07 :

$$D_{pp} = \frac{\pi^2}{2c}\frac{p^2 c_s^2}{B_0^2}\int_{c_s/c}^{1} d\mu \frac{1-\mu^2}{\mu}\left(1-(\frac{c_s}{c\mu})^2\right)^2 \times \int_{k_0}^{k_{cut}} dk W_B(k) k \quad (18)$$

Similarly to the classical second order Fermi mechanism, the acceleration depends on the minimum/dissipation scale of the electromagnetic fluctuations and on the energy density of these fluctuations, being $\int dk W_B k \sim k_{cut}\delta B^2_{k_{cut}}/8\pi$. The dissipation scale is set by the competition between turbulent cascade and collisionless damping. Two situations are considered in the literature:

(i) the collision frequency of thermal particles is $\omega_{ii} < \omega = kc_s$. In this case the damping of the waves is dominated by TTD with thermal particles (electrons) and $k_{cut} \sim 10^4 k_o M_t^4$ (BL07, Miniati 2015, Brunetti 2016). We stress that under these conditions *most* of the turbulent energy is dissipated into the heating of the thermal ICM (see BL07). Assuming a Kraichnan spectrum, this leads to a reacceleration time for CRe :

$$\tau_{acc} = \frac{p^2}{4D_{pp}} \simeq 125(\frac{M_t}{1/2})^{-4}\left(\frac{L_o/300\,\mathrm{kpc}}{c_s/1500\,\mathrm{km\,s^{-1}}}\right) \quad (\mathrm{Myr}) \quad (19)$$

(ii) the collisions between thermal particles in the ICM are fast, $\omega_{ii} > \omega = kc_s$. This is the case where scatterings are mediated by magnetic field perturbations driven by plasma instabilities (eg., Lazarian & Beresnyak 2006, Brunetti & Lazarian 2011b, Santos-Lima et al 2014 and references therein). Contrary to case (i), here the damping of the waves is due to TTD with relativistic particles (CR protons and CRe), turbulence reaches smaller scales and the reacceleration time (for Kraichnan spectrum) is (Brunetti & Lazarian 2011b) :

$$\tau_{acc} \simeq 6(\frac{M_t}{1/2})^{-4}\left(\frac{L_o/300\,\mathrm{kpc}}{c_s/1500\,\mathrm{km\,s^{-1}}}\right)\left(\frac{\mathcal{R}_{CR}}{25}\right) \quad (\mathrm{Myr}) \quad (20)$$

where

$$\mathcal{R}_{CR} = \sum_{i=e,p}\frac{c\int p^4 dp \frac{\partial f_i(p)}{\partial p}}{\rho_{ICM} c_s^2} \quad (21)$$

ρ_{ICM} is the thermal density of the ICM, and $f_i(p)$ is the distribution function of CRs (CRe and CR protons) in the momentum space.

The two acceleration schemes have been used estensively to explain radio halos and mini radio halos in galaxy clusters (BL07, Brunetti & Lazarian 2011a,b, Beresnyak et al 2013, ZuHone et al 2013, Donnert et al 2013, Donnert & Brunetti 2014, Miniati 2015, Pinzke et al. 2015). The main assumptions in these studies is that compressible turbulence is a relevant part of turbulence in the ICM. Challenges of these models due to our poor understanding of the ICM microphysics have been extensively discussed in Brunetti (2016). In particular, it has been shown that an increasingly steeper spectrum of the electromagnetic fluctuations induces a slower acceleration rate essentially because fluctuations are dissipated at larger scales. Recent cosmological simulations suggest that compressive turbulence in the ICM is Burgers-like ($W \propto k^{-2}$). In this case (assuming that velocities and electromagnetic fluctuations follow the same scalings), for typical velocities of the turbulent eddies $\delta V \sim 500 - 800$ km s^{-1} on large scales ($L_0 = 300$ kpc), the efficiency of TTD acceleration drops by about 10 times with respect to that predicted adopting a Kraichnan spectrum (Brunetti 2016, their Fig.1). Under these unfavourable conditions in the collisionless scenario (case (i), Eq.19) TTD would become inefficient and would not provide a valuable scenario for the origin of cluster-scale radio emission. In this case explaining radio halos would require that the ICM behaves mostly collisional (i.e. case (ii), Eq.20) (see Miniati 2015).

As already mentioned the main motivation for the present paper is that large-scale turbulence in the ICM is mainly solenoidal (Miniati 2014). This incompressible turbulence is dissipated into the thermal ICM at a much smaller rate than the compressible part and consequently it provides a previously unexplored, natural energy reservoir for stochastic particle acceleration in the ICM. In this paper we essentially suggest that part of this energy drains into relativistic particles via the interaction with magnetic field lines diffusing in turbulent reconnection. Note that the acceleration mechanism explained in Sect.3.2 do not drain turbulent energy into thermal ICM as these particles do not diffuse on sufficiently large scales. Our mechanism also differs from other models for diffuse radio emission from galaxy clusters that are based on particles-waves interaction via gyro-resonance, where the non-linear coupling between particles and Alfvén waves at very small, resonant, scales $k \sim eBE^{-1}/(\mu \pm V_A/c)$ is used (Ohno et al 2002, Fujita et al 2003, Brunetti et al 2004, Fujita et al 2015). In fact it is unlikely that gyro-resonant acceleration is driven directly by the cascade of incompressible turbulence from large-scales to very small scales because the scale-dependent anisotropies that are developed in the Alfvénic cascade at MHD scales quench the acceleration (Chandran 2000, Yan & Lazarian 2004).

In our model the acceleration drains energy essentially from the Alfvénic motions at the Alfvén scale, l_A. In principle this energy reservoir is large and of the order of the energy flux associated to the turbulence at larger scales, $V_A^3/l_A \sim \delta V^3/L_0$ for Kolmogorov spectrum. As a reference, by considering $\psi \sim 0.2 - 0.5$ and typical conditions for the solenoidal turbulence in the ICM, $M_t^2 \sim 0.3 - 0.8$ and $L_o = 100 - 500$ kpc (consistent with numerical simulations), the acceleration rates (Sect. 4.2) are similar to those expected in the case of collisionless TTD with compressive

turbulence for Kraichnan spectrum (case (i), Eq. 19)[§]. Since collisionless TTD has been successfully applied to radio halos, we conclude that our mechanism may provide a valuable alternative to the mechanisms based on compressible turbulence or that it may play a role in combination with these other mechanisms.

5.2 Dampings and saturation effects

TTD reacceleration by compressible turbulence in the ICM has been calculated considering self-consistently acceleration and turbulent-damping rates (BL07, Brunetti & Lazarian 2011a,b). On the other hand in Sect.3 we have calculated the diffusion coefficient in the particles' momentum space in the test particle regime. If a large fraction of the turbulent energy flux in our model is channelled into CRs, saturation effects become important. Acceleration and turbulent damping, Γ, are connected through detailed balancing :

$$\sum_{i=e,p} \int d^3p E \frac{\partial f_i}{\partial t} = \int d^3k W(\vec{k}) \Gamma(\vec{k}) \quad (22)$$

where the left-hand side of Eq.22 accounts for the energy channelled into CRs and the right-hand side accounts for the energy that is extracted from turbulence via damping; $W(\vec{k})$ is the 3D turbulent spectrum ($W(\vec{k}) = 4\pi k^2 W(k)$ in the isotropic case). Assuming pitch-angle isotropy of CRs, the time-evolution of the CRs momentum distribution in Eq.22 depends on the momentum-diffusion coefficient via :

$$\frac{\partial f_i}{\partial t} = \frac{1}{p^2} \frac{\partial}{\partial p} \left(p^2 D_{pp} \frac{\partial f}{\partial p} \right) \quad (23)$$

and the evolution of the turbulent spectrum is given by (eg. BL07 and references therein) :

$$\frac{\partial W}{\partial t} = \frac{\partial}{\partial k} \left(k^2 D_{kk} \frac{\partial}{\partial k} (\frac{W(k)}{k^2}) \right) - \Gamma W(k) + I(k) \quad (24)$$

where the first and second terms in the right-hand side account for turbulent cascade and damping, respectively, $D_{kk} \sim k^2/\tau_{kk}$ is the diffusion coefficient in the wavenumber space[¶], τ_{kk} is the turbulent cascading-time at scale k^{-1}, and $I(k)$ accounts for the process of injection of turbulence at large scales.

Eqs.22–24 connect acceleration rate, CR energy densities and turbulent damping and cascading. They essentially imply that the increase of the energy density of CRs with time produces a stronger damping, with the consequence that the turbulent spectrum is gradually suppressed and that acceleration is reduced. In this regime full Fokker-Planck time-dependent calculations, combined with the modeling of the evolution of the turbulent spectrum, are necessary for a correct evaluation of the acceleration process (see e.g. Brunetti et al 2004, Brunetti & Lazarian 2011b for examples of calculations in the ICM). These saturation effects also limit the applicability of the approach used in Sect.4.2, that is based on the scaling of the (spectral) analysis in compressive turbulent acceleration to the case of (incompressible) turbulent reconnection.

In our acceleration model the turbulent eddies on scale $\sim l_A$ are the most important ones. Consequently the importance of saturation effects can be evaluated by comparing damping and turbulent cascade at these scales: if damping rate is smaller than the rate of turbulent cascade, $\tau^{-1}_{l_A l_A} \sim V_A l_A^{-1}$, the turbulent spectrum is not modified and saturation effects are not important. This is the case when the energy flux of turbulent cascade at the Alfvén scale, $\sim \rho_{ICM} V_A^3 l_A^{-1}$, is much larger than the energy flux that is channeled into CRs. The two quantities can be connected via :

$$\rho_{ICM} V_A^3 l_A^{-1} \eta_{CR} \sim c \int d^3p \frac{1}{p} \frac{\partial}{\partial p} \left(p^2 D_{pp} \frac{\partial f}{\partial p} \right) \quad (25)$$

where η_{CR} is the fraction of turbulent energy flux that is transferred into CRs by our mechanism, and D_{pp} is given in Eq.8. The limit $\eta_{CR} \to 1$ corresponds to strong damping. In fact this limit constrains the minimum value of ψ that is allowed in test-particle calculations (i.e. neglecting saturation/damping effects) of our model. From Eqs.8 and 25 this is :

$$\psi_{min} \sim \left(\frac{5}{2} \beta_{pl} \frac{V_A}{c} \frac{\epsilon_{CR} \mathcal{S}_{CR}}{\rho_{ICM} c_s^2} \right)^{1/3} \quad (26)$$

where we define :

$$\mathcal{S}_{CR} = \frac{\sum_{i=e,p} \int d^3p \frac{1}{p} \frac{\partial}{\partial p} (p^4 \frac{\partial f_i}{\partial p})}{\sum_{i=e,p} \int d^3p f_i(p) p} \quad (27)$$

As expected, limits on ψ depend on the energy density of CRs in the ICM. Theoretical reasons suggest that CR protons are the most important CR component in galaxy clusters (BJ14 for review). In the recent years gamma-ray and radio observations allowed to constrain the energy density that is associated to CR protons in the central Mpc-regions of galaxy clusters, $\epsilon_{CR} <$ few $0.01 \times \epsilon_{ICM}$ (eg., Ackermann et al 2010, 2014, Zandanel & Ando 2014, Brunetti et al 2007, 2008, BJ14 for review). If we use these reference values, Eq.26 basically implies $\psi > 0.1$.[‖] This limit on ψ is fully consistent with the values used/derived in Sect.4.2 to explain cluster-scale radio emission.

Interestingly for $\psi \sim 0.1$ the turbulent velocities that are necessary to explain radio halos are still significant $\delta V_o > 100$ km/s (for example > 90 and $> 140 (L_o/100)^{1/3} (n_{ICM}/10^{-3})^{-1/6}$ km/s for the radio halos in Coma and Bullet clusters, respectively, see Sect.4). This essentially sets the level of the minimum turbulent broadening of the profile of X-ray lines that is expected in our model. Non detection of such a broadening with future X-ray spectrometers, for example with ATHENA, will rule out our model under the conditions explored in this paper (namely fast diffusion approximation and $\Delta p \ll p$, Sect.3.2)[★★].

[§] this is also equivalent to acceleration rates expected in the case of collisional TTD ((ii), eq.20) assuming Burgers–like spectrum of turbulence, or in the case of Kraichnan spectrum assuming smaller values of the turbulent Mach number, $M_t^2 \sim 0.05 - 0.1$

[¶] more specifically it is $\tau_{kk} = k^3 / \frac{\partial}{\partial k} (D_{kk} k^2)$

[‖] On the other hand, if we consider only CRe in the ICM, or an *ad hoc* situation where CR protons are not accelerated by our mechanism, it is $\mathcal{S}_{CRe} \epsilon_{CRe} \sim 10^{-5} - 10^{-4} \rho_{ICM} c_s^2$ and essentially $\psi > 0.02$.

[★★] alternatively it will require an *ad hoc* situation where CRp are not accelerated efficiently by our mechanism

5.3 Reacceleration of CR protons

As a final remark we point out that in principle our mechanism reaccelerate also CR protons that will accumulate their energy more efficiently than CRe (because CRp are subject to less efficient energy losses, see BJ14 for a review). The energy density accumulated by CR protons in a reacceleration time Δt will be :

$$\rho_{ICM} V_A^3 l_A^{-1} \langle \eta_{CR} \rangle_{\Delta t} \Delta t \approx \Delta t \int d^3p E \frac{\partial f_p}{\partial t} \sim \delta\epsilon_{CR} \quad (28)$$

where $\langle \eta_{CR} \rangle_{\Delta t} \Delta t = \int_0^{\Delta t} \eta_{CR}(t) dt$.
In practice CR protons will release part of this energy due to losses in Gyr-time scales. In a few Gyrs CR protons will be also advected and transported by large-scale motions on scales larger than the relevant turbulent scales and thus energy will be redistributed on large-scales decreasing $\delta\epsilon_{CR}$. Nevertheless we can use Eq.28 under the condition $\delta\epsilon_{CR} < \epsilon_{CR}$ to derive a (order of magnitude) limit on Δt; it is useful also to check if our calculations in the case of radio halos are self-consistent. This is (from Eqs.25, 8 and 28) :

$$\Delta t \sim \frac{c}{3} \frac{l_A}{V_A^2} \frac{\epsilon_{CR}(\delta\epsilon_{CR}/\epsilon_{CR})}{\langle \epsilon_{CR}(t) \mathcal{S} \rangle_{\Delta t}} \psi^3 \quad (29)$$

where $l_A = M_t^{-3} L_o (V_A/c_s)^3$. At this point Eq.29 can be combined with the Mach number that is requested to generate radio halos with observed synchrotron steepening frequency ν_o (under the minimal condition $B \sim B_{cmb}/\sqrt{3}$, Eq. 16) :

$$\Delta t \sim \left(\frac{\nu_o(GHz)}{3} \frac{7}{\xi} \right)^{-\frac{1}{2}} (1+z)^{-\frac{3}{2}} \frac{\epsilon_{CR}(\delta\epsilon_{CR}/\epsilon_{CR})}{\langle \epsilon_{CR}(t) \mathcal{S} \rangle_{\Delta t}} \ \text{(Gyr)} \quad (30)$$

where typically $\epsilon_{CR}/\langle \epsilon_{CR}(t) \mathcal{S} \rangle_{\Delta t} \gtrsim 1$. We thus conclude that radio halos observed at GHz frequencies can be generated by our mechanism for Gyrs. These time-scales are comparable to the life-times of radio halos evaluated from statistical analysis (eg. Brunetti et al 2009, BJ14) suggesting that the exploratory (test-particle) calculations in Sect.3.2 and 4 provide a good approximation. A reliable modeling of the acceleration process for longer acceleration periods (or for radio halos with spectra extending to $\nu_o \gg$ few GHz) requires full Fokker-Planck time-dependent calculations combined with numerical simulations of clusters (including CRs transport).

6 SUMMARY

We suggest that relativistic particles diffusing in super-Alfvenic incompressible turbulence gain energy due to the statistical interaction with field lines in regions of magnetic reconnection and turbulent dynamo. In view of large-scale turbulence being present in the ICM we assume a scheme based on turbulent reconnection and assume that MHD turbulence provides a good guide as far as reconnection is considered. We calculate the acceleration rate in the *fast* diffusion regime and in the limit $\Delta p \ll p$. Under these conditions the mechanism is essentially a second-order Fermi.
In this exploratory paper we account for the interaction between magnetic field lines and CRe on large scales, ∼0.1-1 kpc, assuming transport properties and turbulent scalings that follow from MHD turbulence. Additional kinetic effects on smaller-scales may affect the physics of reconnection and CRe transport and acceleration. For this reason we consider CRe mfp as a free parameter that is however bounded by the combination of basic constraints, including the confinement of CRe (Sect.3.2), the interaction with large-scale fields (Sect. 3.2) and indirect considerations on the turbulent energy flux that is available (Sect.5).
We propose that the mechanism may play a role for the origin of radio halos and large-scale diffuse emission in galaxy clusters. In fact, assuming reliable conditions in the ICM we have shown that the expected reacceleration rate is similar to that of classical reacceleration models proposed for radio halos, provided that the CRe mfp is a fraction $\sim 0.1 - 0.5$ of the MHD scale. Smaller values of the mfp would make the mechanism even more efficient, however in this case saturation/damping effects (Sect. 5.2) should become important invalidating the test-particle approach adopted in our paper and deserve future studies.
Similarly to previous reacceleration models the diffusion coefficient in the momentum space is $D_{pp} \propto p^2$ and thus, in principle all previous results based on solutions of Fokker-Planck equations can be easily extended to our case. However our approach differs from these previous models because it is based on the incompressible part of the turbulence and because it is mediated by turbulent reconnection and dynamo. According to current numerical cosmological simulations incompressible turbulence in the ICM is found to be dominant, super-Alfvenic and *quasi*–sonic and thus the new mechanism explored in our paper appears particularly appealing. Interestingly in our mechanism the conditions that are necessary to generate radio halos have unavoidable consequences on the broadening of the profile of X-ray lines, allowing a test of model assumptions with forthcoming X-ray calorimeters (ASTRO-H, ATHENA).
This is an exploratory paper.
One of the critical points is the particles mfp. The combined effect of super-Alfvenic motions and resonant mirroring with pseudo Alfven modes constrains the mfp ∼ a fraction of the MHD scale. However in a more general situation additional scattering agents induced by additional turbulent components may reduce the mfp; this might have the potential to increase the acceleration rate.
Another critical point is the assumption of turbulent reconnection scheme. The basic assumption here is that reconnection is part of the MHD cascade. This appears quite natural in the ICM given the presence of large-scale turbulence that can be driven at large scales in merging clusters and given the observed connection between mergers and non-thermal emission from galaxy clusters. Other schemes, such as tearing reconnection, do not invalidate *per se* our reacceleration scheme, provided that reconnection and dynamo are still triggered by large-scale motions. This however requires an extension of our modelling.
Calculations in this paper focus on the hypothesis of fast-diffusion regime and $\Delta p \ll p$ (Sect. 3.2). Numerical simulations can be used to extend this exploratory study to the situation $\Delta p \sim p$, in which case the mechanism is expected to differ significantly from a second order Fermi. Simulations will also allow to calculate the acceleration rate under more realistic configurations of reconnection and dynamo regions.
Finally it is worth to mention that in our model we focus on the reacceleration of CRe. Also CR protons, if present, will

be reaccelerated by our mechanism. As a sanity-check we have shown that, assuming the physical parameters that are requested to explain radio halos, the energy budget of CR protons resulting from a reacceleration period comparable to the life-time of halos is consistent with current limits from γ-ray observations. At this point, since reacceleration rates and diffusion coefficient, $D_{pp} \propto p^2$, in our model are equivalent/similar to those in lepto-hadronic reacceleration models where CR protons and their secondary particles have been explicitly taken into account (eg. Brunetti & Lazarian 2011a, Brunetti et al 2012, Pinzke et al 2015), also the conclusions of these previous works can be extended to our picture.

7 ACKNOWLEDGMENTS

We thank the referee for useful comments that have improved the presentation of the paper. GB and AL acknowledge support from the Alexander von Humboldt Foundation and discussions with Prof. R. Schlickeiser. GB acknowledges support from PRIN-INAF 2014, AL acknowledges support from NASA grant NNX14AJ53G.

REFERENCES

Ackermann, M., Ajello, M., Allafort, A., et al. 2010, ApJ, 717, L71
Ackermann, M., Ajello, M., Albert, A., et al. 2014, ApJ, 787, 18
Beresnyak, A. 2013, arXiv:1301.7424
Beresnyak, A., Yan, H., & Lazarian, A. 2011, ApJ, 728, 60
Beresnyak, A., Xu, H., Li, H., & Schlickeiser, R. 2013, ApJ, 771, 131
Bhattacharjee, A. 2004, Annual Rev. of Astronomy & Astrophysics, 42, 365
Brüggen, M., & Vazza, F. 2015, ASSL, 407, 599
Birn, J., Drake, J. F., Shay, M. A., et al. 2001, Journal of Geophysical Research, 106, 3715
Brunetti, G. 2016, Plasma Physics and Controlled Fusion, 58, 014011
Brunetti, G., Setti, G., Feretti, L., & Giovannini, G. 2001, MNRAS, 320, 365
Brunetti, G., Blasi, P., Cassano, R., & Gabici, S. 2004, MNRAS, 350, 1174
Brunetti, G., Venturi, T., Dallacasa, D., et al. 2007, ApJ, 670, L5
Brunetti, G., Lazarian A., 2007, MNRAS, 378, 245
Brunetti, G., Cassano, R., Dolag, K., Setti, G. 2009, A&A, 507, 661
Brunetti, G., & Lazarian, A. 2011a, MNRAS, 410, 127
Brunetti, G., & Lazarian, A. 2011b, MNRAS, 412, 817
Brunetti, G., Blasi, P., Reimer, O., et al. 2012, MNRAS, 426, 956
Brunetti, G., Rudnick, L., Cassano, R., et al. 2013, A&A, 558, A52
Brunetti, G., & Jones, T. W. 2014, International Journal of Modern Physics D, 23, 1430007
Carilli, C.L., Taylor, G.B. 2002, Annual Rev. of Astronomy & Astrophysics, 40, 319
Cassano, R., & Brunetti, G. 2005, MNRAS, 357, 1313
Cassano, R., Brunetti, G., Röttgering, H.J.A, Brüggen, M. 2010, A&A, 509, A68
Cassano, R., Ettori, S., Brunetti, G., et al. 2013, ApJ, 777, 141
Chandran, B. D. G. 2000, Physical Review Letters, 85, 4656
Cuciti, V., Cassano, R., Brunetti, G., Dallacasa, D., Kale. R., Ettori, S., Venturi, T. 2015, arXiv:1506.03209
Daughton, W., Roytershteyn, V., Karimabadi, H., et al. 2011, Nature Physics, 7, 539
de Gouveia dal Pino, E. M., & Lazarian, A. 2005, A&A, 441, 845
Donnert, J., Dolag, K., Brunetti, G., & Cassano, R. 2013, MNRAS, 429, 3564
Donnert, J., Brunetti, G., 2014, MNRAS, 443, 3564
Drake, J. F., Swisdak, M., Che, H., & Shay, M. A. 2006, Nature, 443, 553
Drake, J. F., Opher, M., Swisdak, M., & Chamoun, J. N. 2010, ApJ, 709, 963
Drake, J. F., Swisdak, M., & Fermo, R. 2013, ApJ, 763, L5
Drury, L. O'C., 2012, MNRAS, 422, 2474
Eyink, G. L. 2011, Physical Review E, 83, 056405
Eyink, G., Vishniac, E., Lalescu, C., et al. 2013, Nature, 497, 466
Eyink, G. L. 2015, ApJ, 807, 137
Ettori, S., Pratt, G.W., de Plaa, J., et al. 2013, arXiv:1306.2322
Feretti, L., Giovannini, G., Govoni, F., & Murgia, M. 2012, Astronomy & Astrophysics Rev., 20, 54
Fisk, L. A. 1976, Journal of Geophysical Research, 81, 4633
Fujita, Y., Takizawa, M., & Sarazin, C. L. 2003, ApJ, 584, 190
Fujita, Y., Takizawa, M., Yamazaki, R., Akamatsu, H., Ohno, H. 2015, ApJ, 815, 116
Giannios, D. 2013, MNRAS, 431, 355
Kadowaki, L. H. S., de Gouveia Dal Pino, E. M., & Singh, C. B. 2015, ApJ, 802, 113
Karimabadi, H., & Lazarian, A. 2013, Physics of Plasmas, 20, 112102
Khiali, B., de Gouveia Dal Pino, E. M., & del Valle, M. V. 2015, MNRAS, 449, 34
Kitayama, T., Bauts, M., Markevitch, M., et al. 2014, arXiv:1412.1176
Kowal, G., Lazarian, A., Vishniac, E. T., & Otmianowska-Mazur, K. 2009, ApJ, 700, 63
Kowal, G., de Gouveia Dal Pino, E. M., & Lazarian, A. 2011, ApJ, 735, 102
Kowal, G., de Gouveia Dal Pino, E. M., & Lazarian, A. 2012, Physical Review Letters, 108, 241102
Lalescu, C. C., Shi, Y.-K., Eyink, G. L., et al. 2015, Physical Review Letters, 115, 025001
Lazarian A., Vishniac E.T., 1999, ApJ, 517, 700 (LV99)
Lazarian, A., & Beresnyak, A. 2006, MNRAS, 373, 1195
Lazarian, A., & Opher, M. 2009, ApJ, 703, 8
Lazarian, A., & Desiati, P. 2010, ApJ, 722, 188
Lazarian, A., & Brunetti, G. 2011, MmSAIt, 82, 636
Lazarian, A., Eyink, G. L., Vishniac, E. T., & Kowal, G. 2015, ASSL, 407, 311
Le Roux, J.A, Zank G.P, Webb G.M., Khabarova O. 2015, ApJ, 801, 112
Liang, H., Hunstead, R. W., Birkinshaw, M., & Andreani, P. 2000, ApJ, 544, 686
Longair, M. S. 2011, *High Energy Astrophysics*, Cambridge, UK: Cambridge University Press, 2011
Loureiro, N. F., Schekochihin, A. A., & Cowley, S. C. 2007, Physics of Plasmas, 14, 100703
Lyubarsky, Y. E. 2003, MNRAS, 345, 153
Lyutikov, M., & Blandford, R. 2003, arXiv:astro-ph/0312347
Macario, G., Venturi, T., Intema, H. T., et al. 2013, A&A, 551, A141
Makwana, K.D, Zhdankin V., Li, H., Daughton, W., Cattaneo, F. 2015, Physics of Plasmas, 22, 042902
Marchegiani, P., & Colafrancesco, S. 2015, MNRAS, 452, 1328
Mertsch , P. 2011, Journal of Cosmology and Astroparticle Physics, 12, 010
Miniati, F. 2014, ApJ, 782, 21
Miniati, F. 2015, ApJ, 800, 60
Miniati, F., & Beresnyak, A. 2015, Nature, 523, 59
Ng, J., Huang, Y.-M., Hakim, A., et al. 2015, arXiv:1511.00741
Ohno, H., Takizawa, M., & Shibata, S. 2002, ApJ, 577, 658
Oishi, J. S., Mac Low, M.-M., Collins, D. C., & Tamura, M. 2015, ApJ, 806, L12

Owen, F. N., Rudnick, L., Eilek, J., et al. 2014, ApJ, 794, 24
Parker, E. N. 1957, Journal of Geophysical Research, 62, 509
Petrosian, V. 2001, ApJ, 557, 560
Petrosian, V., & East, W. E. 2008, ApJ, 682, 175
Petschek, H. E. 1964, NASA Special Publication, 50, 425
Pinzke, A., Oh, S. P., & Pfrommer, C. 2015, arXiv:1503.07870
Porter, D. H., Jones, T. W., & Ryu, D. 2015, ApJ, 810, 93
Ryu, D., Kang, H., Cho, J., & Das, S. 2008, Science, 320, 909
Santos-Lima, R., de Gouveia Dal Pino, E. M., Kowal, G., et al. 2014, ApJ, 781, 84
Schlickeiser, R., *Cosmic ray astrophysics*, Springer (2002)
Schlickeiser, R. 1984, A&A, 136, 227
Schlickeiser, R., & Miller, J. A. 1998, ApJ, 492, 352
Shay, M. A., Drake, J. F., Denton, R. E., & Biskamp, D. 1998, Journal of Geophysical Research, 103, 9165
Shimwell, T. W., Brown, S., Feain, I. J., et al. 2014, MNRAS, 440, 2901
Sironi, L., & Spitkovsky, A. 2014, ApJ, 783, L21
Sweet, P. A. 1958, Electromagnetic Phenomena in Cosmical Physics, 6, 123
Uzdensky, D. A., Loureiro, N. F., & Schekochihin, A. A. 2010, Physical Review Letters, 105, 235002
Vazza F., Brunetti G., Gheller C., Brunino C., Brüggen M. 2011, A&A, 529, A17
Venturi, T. 2011, MmSAIt, 82, 499
Yan, H., & Lazarian, A. 2004, ApJ, 614, 757
Yan, H., & Lazarian, A. 2008, ApJ, 673, 942
Zandanel, F., & Ando, S. 2014, MNRAS, 440, 663
Zhang, B., & Yan, H. 2011, ApJ, 726, 90
Zank, G. P., le Roux, J. A., Webb, G. M., Dosch, A., & Khabarova, O. 2014, ApJ, 797, 28
ZuHone, J. A., Markevitch, M., Brunetti, G., & Giacintucci, S. 2013, ApJ, 762, 78